

Optical Properties of Some Fluorinated Poly(1,3,4-Oxadiazole-Ether)s in Homogeneous and Heterogeneous Media. Changes Induced by SnO₂, NiO and SnO₂/NiO Mixed-Oxide Nanoparticles

Mihaela Homocianu¹ · Anton Airinei¹ · Alina Mirela Ipate¹ · Petronela Pascariu Dorneanu¹ · Corneliu Hamciuc¹

Received: 4 July 2015 / Accepted: 20 October 2015 / Published online: 30 October 2015
© Springer Science+Business Media New York 2015

Abstract Optical characteristics of some fluorinated poly(1,3,4-oxadiazole-ether)s in presence of SnO₂, NiO and SnO₂/NiO mixed-oxide nanoparticles (NPs) was investigated. The interactions between polymers and metal oxide NPs were studied by steady-state UV-Vis absorption and fluorescence spectroscopy techniques. The absorption and fluorescence signals of all investigated polymers was modified by presence of both pure and mixed-oxide nanoparticles. The moderate values of Stern-Volmer quenching constant and non-linear trend of Scott plot indicate the less affinity between metal oxide NPs and polymers. The solvation behavior of some fluorinated poly(1,3,4-oxadiazole-ether)s in chloroform–N,N-dimethylformamide and N,N-dimethylformamide–dimethylsulfoxide mixtures was discussed.

Keywords SnO₂, NiO and SnO₂/NiO nanoparticles · Fluorinated poly(1,3,4-oxadiazole-ether)s · Absorption and fluorescence spectra · Heterogeneous media

Introduction

Generally, the polyheterocyclic ethers have a specially interest in research due to their structure and unique combination of properties (relatively easy solution processability, chemical stability, flame resistance, degrad-

ability and biocompatibility), that makes them good candidates for various applications, in microelectronics, optoelectronics, advanced telecommunications, sensors or other related fields [1–3]. Also, they are characterized by high electron affinity [4].

For the numerous solutes have been tested and are published the papers regarding the solvent effects on the photophysical behavior. However, the effect of heterogeneous medium (mixed solvents) on the photochemical and photophysical behavior has been less investigated. In the literature was published papers in which the intermolecular interactions from mixed solvents are discussed in terms of the preferential solvation and less is approached the quantitative analysis of the effect of the environment (distribution of the solvents from system as against solute, the correlation of electro-optical parameters of medium with spectral data of the solute). The tailored heterogeneous media (mixed solvents) have the advantages that allows to combining the properties of pure solvents, creating thus new systems with desirable and high physical characteristics (solubility, viscosity, dielectric constant or refractive index). Also, working in mixed solvents can choose suitable solvents and proportions so that the new created system to be friendlier with the environment.

Tin oxide nanoparticles (SnO₂ NPs) with optical [5], electrochemical, biological activities [6, 7] and photocatalytic properties [8] are extensively used as solar cells, solid-state sensors and optical electronic devices [9]. Mixing metal oxide nanoparticles (e.g. SnO₂/NiO) which have different chemical, magnetic and/or optical properties can be obtained newly materials with enhanced characteristics and different potential applications.

Generally, the presence of the metal nanoparticles in a system can influence the optical properties of molecules by

✉ Mihaela Homocianu
michalupu@yahoo.co.uk

¹ “Petru Poni” Institute of Macromolecular Chemistry, 41A Grigore Ghica Voda Alley, 700487 Iasi, Romania

several processes, such as the plasmon resonance [10], the modification of the radiative decay rate of the molecule [11] and the increase of the fluorescence emission by nanoparticle scattering [12]. The fluorescence intensity of the solutes (fluorophores) in presence of metal NPs can enhance or quench depending on the lot of factors, like the molecular dipole orientation of the fluorophores, the solute-nanoparticle separation and nanoparticles surface and size [13].

The control of the relation between surface plasmon resonance of the metal nanoparticles and complete quenching or extensive enhancement of the fluorescence signal present an real interest for synthesis of the new nanoparticle-fluorophores architectures with optimal fluorescence characteristics for different applications. Also, heterogeneous media (mixed liquids/solvents) and presence of mixed metal oxide nanoparticles can have cumulative effects in development of the new systems with desirable optical characteristics for specific applications.

In this work, the influences of pure and mixed metallic nanoparticles on the spectroscopic (fluorescence and absorption) properties of some fluorinated poly(1,3,4-oxadiazole-ether)s were investigated. Our results show that varying concentrations of metal nanoparticles, the polymer solutions exhibit remarkable differences in absorption and fluorescence signals. Also, we analyze the photophysical behavior of sample 9F-Ox in heterogeneous media (chloroform–N,N dimethylformamide (CHCl₃-DMF) and N,N dimethylformamide-dimethylsulfoxide (DMF-DMSO) mixtures) by absorption and emission steady state spectroscopic methods, as a function of the solvent composition. The changes in spectral data of the probe with variations in the media compositions have been analyzed in terms of preferential solvation parameters.

Experimental Section

Materials and Methods

The investigated fluorinated poly(1,3,4-oxadiazole-ether)s were synthesized by our research group [14, 15]. Also, the metal oxide nanoparticles used in this study were prepared according to a published procedure [16, 17].

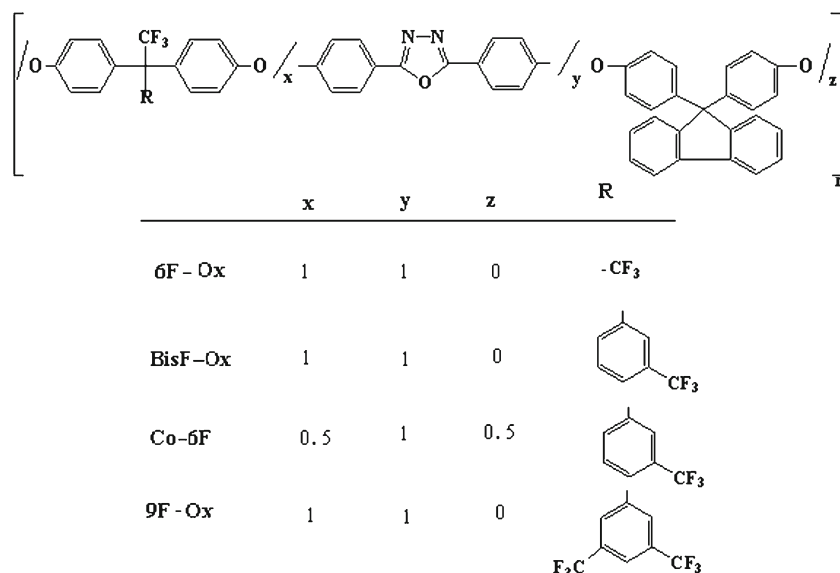
The molecular structures of studied polymer are presented in Fig. 1.

The solvents used in the present study were of spectroscopic grade. The absorption and fluorescence spectra of investigated samples were measured using a Shimadzu 3600 UV/Vis/NIR spectrophotometer and Perkin Elmer LS 55 spectrofluorimeter. The effects of pure and mixed metal nanoparticles on the optical properties of investigated fluorinated poly(1,3,4-oxadiazole-ether)s was studied by mixing 2.5 mL solution containing appropriate concentration of polymer (1×10^{-5} M) with successive volume of solution of colloidal SnO₂, NiO or SnO₂/NiO oxide nanoparticles as quenchers. For fluorescence measurements the 300 nm was used as the excitation wavelength.

The following concentrations of metal oxide nanoparticles were used: 4.97×10^{-3} M for SnO₂; 1.03×10^{-4} M for NiO and 1.15×10^{-3} M for SnO₂/NiO mixed oxide NPs. All the measurements were made at room temperature. The quantity of quencher added depends on the polymer sensitivity.

Preferential solvation of 9F-Ox was investigated in CHCl₃-DMF and DMF-DMSO solvent mixtures. These binary liquid systems were prepared by mixing the solvents in variable proportions (1:5, 2:4, 3:3, 4:2 and 5:1) to a final total volume of 6 mL. For resulting solutions the absorption and emission spectra were recorded.

Fig. 1 Chemical structures of studied compounds



Results and Discussion

Changes Induced by Presence of SnO₂, NiO and SnO₂/NiO Mixed-Oxide Nanoparticles Absorption Investigations

The absorption spectrum of the SnO₂ and NiO oxide nanoparticles in chloroform solution has a maximum in the range 270–380 nm (Fig. 2). These absorption bands result from interactions of free electrons confined of metallic nanoparticles with incident electromagnetic radiation.

The steady-state spectral characteristics (the shape of spectra, position of the absorption and emission maximum wavelengths, Stokes shifts values, solvatochromism) of investigated polymer in various pure solvents and three mixed solvent systems (chloroform–N,N-dimethylformamide (CHCl₃–DMF), chloroform–dimethyl sulfoxide (CHCl₃–DMSO) and dimethylformamide–dimethyl sulfoxide (DMF–DMSO)) have been studied in previous papers [14, 15].

Changes induced on the absorbance properties of BisF-Ox in CHCl₃ solution by presence of SnO₂/NiO nanoparticles are shown in Fig. 3. The observed absorption band shows a minor blue shift, upon adding more quantity (500–1100 μL) of SnO₂/NiO NPs in system comparatively of absorption maximum of the pure BisF-Ox in chloroform solution. This blue shift upon the addition of oxide metallic NPs can be due to the changes that appear in the refractive index of the system medium. The absorbance of all investigated polymer solution increases with an increase in the SnO₂/NiO NPs concentration from suspension (Fig. 3). This can be attributed to enhanced local photon density in the vicinity of the solute fluorophore, as consequently of the interaction between incident light and surface plasmon of the metallic NPs [18] or to transfer energy from the metal NPs to the fluorophores. Also, it is observed a change in optical density upon adding different concentrations

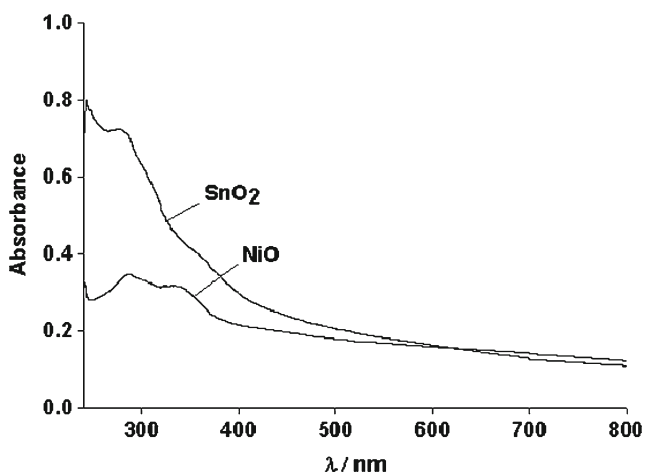


Fig. 2 Absorption spectrum of the SnO₂ and NiO oxide NPs in chloroform solution

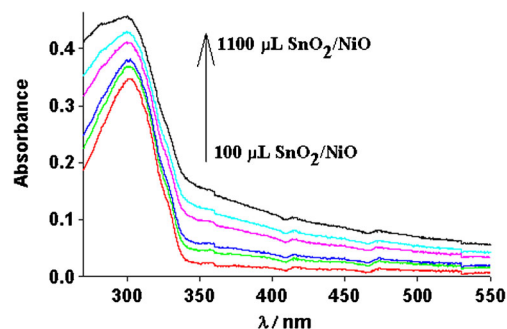


Fig. 3 Absorption spectra of pure BisF-Ox in chloroform and upon adding the tin oxide nanoparticles

of nanoparticles. This behavior was observed for all investigated samples in presence of SnO₂ or NiO nanoparticles.

Fluorescence Emission Studies

Figure 4 shows the fluorescence spectra of pure BisF-Ox in CHCl₃ and in presence of the variable concentrations of tin oxide nanoparticles (SnO₂ NPs) in chloroform suspension. The maxima emission wavelengths of the sample BisF-Ox could be observed at 356 and 372 nm upon excitation with the wavelengths of the maximum absorbance and a shoulder on the longer wavelength side, at 455 nm.

Adding metal oxide nanoparticles in polymer solutions, the positions of the maximum emission wavelength remained unchanged but the fluorescence intensity of the system decreases as the concentration of tin oxide nanoparticles increases. This is due to the interactions between NPs and polymer chains. The emission spectra of pure BisF-Ox in CHCl₃ (Fig. 4) and the absorption spectrum of SnO₂ NPs in CHCl₃ (Fig. 2), this may indicate the absence of Forster energy transfer between polymer and tin oxide nanoparticles. In this case the surface (high surface is induced by presence of nanoparticles) has strongly effect in the interactions of polymer with nanoparticles [19]. The quenching effect of the fluorescence signal can be a consequence of the fact that with increase in the concentration of SnO₂ nanoparticles, more dye molecules were adsorbed on SnO₂ surface [20].

The measured emission intensities show a quenching effect produced by presence of all metallic nanoparticles (SnO₂, NiO and SnO₂/NiO) in chloroform solutions for all investigated samples.

The fluorescence quenching follows the Stern-Volmer (SV) equation given below [21]:

$$\frac{I_0}{I} = 1 + K_{SV} \cdot [C_Q] \quad (1)$$

where, I_0 and I are the fluorescence intensity in the absence and presence of the quencher; K_{SV} is the Stern-Volmer constant and $[C_Q]$ is the concentration of the quencher molecules.

The Stern–Volmer plots are considered as linear (see Fig. 5), which suggests that only one type of quenching occurs

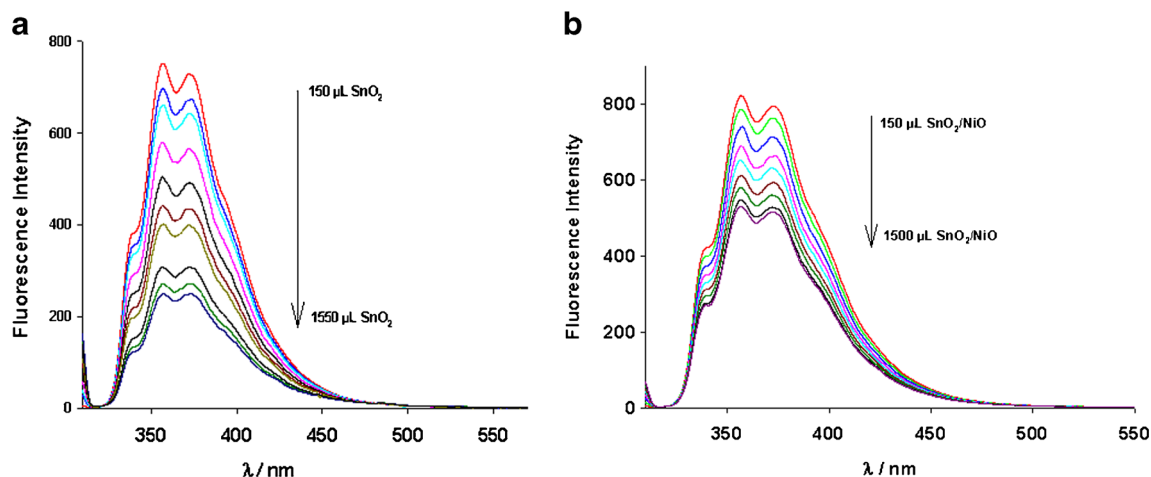


Fig. 4 Emission spectra of pure BisF-Ox in CHCl_3 and upon adding SnO_2 nanoparticles **a** and SnO_2/NiO mixed-oxide nanoparticles **b**. Excitation wavelength was 300 nm

in the system and no complex was formed between the fluorophore and metal oxide nanoparticles. The slope of this linear dependence is called the Stern–Volmer constant. The calculated K_{SV} constants and the correlation coefficient, R^2 for all investigated systems were listed in Table 1.

The efficiency of the quenching of the analyzed polymers was evaluated using the following equation:

$$\% \text{quenching} = \left(\frac{I_0 - I}{I_0} \right) * 100 \quad (2)$$

The obtained values of the quenching efficiency were listed in Table 1. Comparing the effect of SnO_2 and SnO_2/NiO mixed nanoparticles it is observed that a greater reduction of intensity is seen when SnO_2 NPs was added in system, for sample BisF-Ox in chloroform suspension (see Table 1 and Figs. 4(a) and (b)). The R^2 coefficient of the determinations gives information about the goodness fit of the data to the Stern–Volmer model.

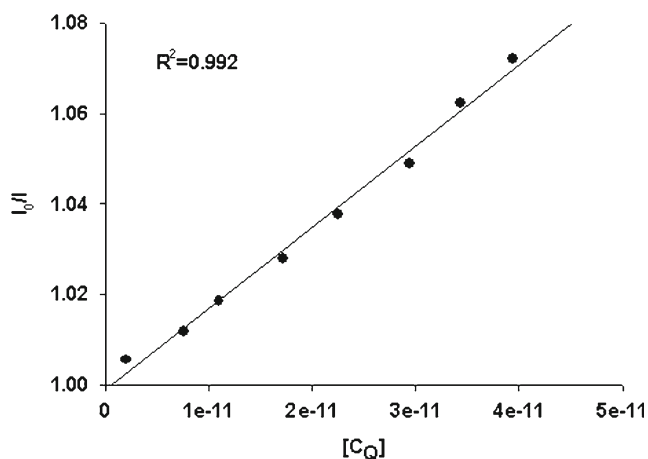


Fig. 5 Stern–Volmer plot for fluorescence quenching of BisF-Ox by NiO nanoparticles, in chloroform solution

Also, from plot of the quenching efficiency (% quenching, Table 1) function of the ratio between the molar concentrations of donor and acceptor ($x = [C_D]/[C_A]$) [22], we can observe that for sample BisF-Ox in presence of SnO_2 (Fig. 6), the efficiency of the quenching increases easily (exponentially) with decreasing in x values. This ratio (x) describes the distribution of the donor (polymer) and acceptor (metal oxide NPs) from investigated system at different contents of the metal oxide nanoparticles. The Coulomb attraction forces are responsible for different values of x (Table 1) [23]. The maximum values of quenching efficiency (36.71 %) were obtained for the ratio of molar concentration is equal to 4.65.

Generally, the investigated metal oxide NPs systems have a moderate quenching efficiency for fluorinated poly(1,3,4-oxadiazole-ether)s fluorescence (excepting effect of SnO_2 on emission intensity of BisF-Ox).

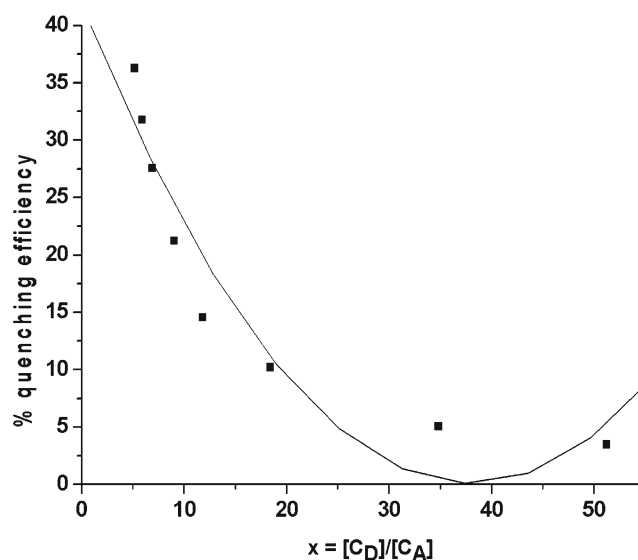


Fig. 6 Plot of dependence of the quenching efficiency of BisF-Ox with donor/acceptor ratio ($[C_D]/[C_A]$). The solid line is fitting data in first order exponential decay

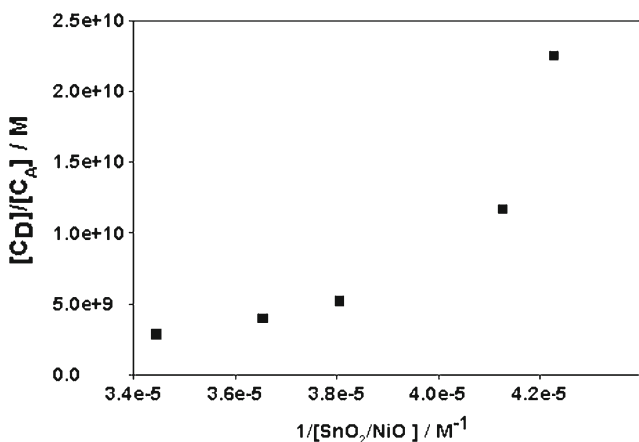


Fig. 7 Plot of $[C_D]/[C_A]$ versus $1/[C_Q]$, for sample BisF-Ox in presence of SnO_2/NiO

The existence of a single mechanism (linear Stern-Volmer plots) of the quenching process is confirmed also by the results obtained from absorption changes upon adding metal oxide NPs. Thus, using, the Scott's equation (Eq. (3)), we plotted the $[C_D]/[C_A]$ versus $1/[C_Q]$, for sample BisF-Ox in presence of SnO_2/NiO (Fig. 7). The deviation from the linear nature of this plot suggests a weak association between the investigated sample and SnO_2/NiO mixed NPs [24].

$$[C_D][C_A]/A = (1/\epsilon)[C_A] + 1/K \tag{3}$$

where $[C_D]$ is the concentration of polymer (donor); $[C_A]$ concentration of NPs (acceptor); A is the absorbance of the polymer/NPs system; ϵ is the molar absorptivity and K is the association constant.

Photobehaviour of Sample 9F-Ox in Heterogeneous Media

Impact of heterogeneous media on the photophysical behavior was investigated for sample 9F-Ox in CHCl_3 -DMF and DMF-DMSO liquid mixtures. In previous study [14], for samples 6F-Ox and BisF-Ox (Table 1), we observed that after addition of successively small amounts of the polar solvents (DMF or DMSO) in CHCl_3 -DMF and CHCl_3 -DMSO mixtures, the absorption and photoluminescence signals are progressively quenched. Thus, the changes in the composition of the medium induce a monotonically quenching effect of the optical (absorbance and emission) signals, but without strongly differences in the profile of the absorption and emission spectra.

The absorption (inset plot) and emission electronic spectra of sample 9F-Ox in DMF-DMSO mixtures are presented in Fig. 8. From this picture we can observe that the profile of the absorption and emission spectra

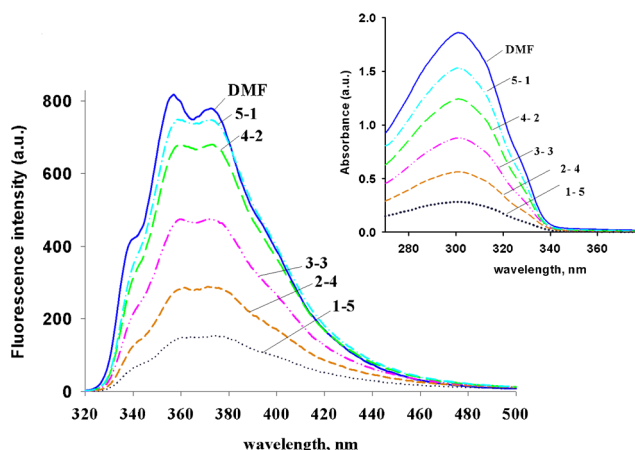


Fig. 8 Fluorescence spectra of sample 9F-Ox in pure DMF and DMF-DMSO mixtures. The inset shows the absorption spectra of 9F-Ox in pure DMF and DMF-DMSO mixtures

of sample 9F-Ox in DMF-DMSO mixtures are similar with those in CHCl_3 -DMF [25].

The absorption and emission energies in mixed liquids (see Table 2) are calculated by considering the contribution of each solvent weighted by its volume fraction, according to following relation:

$$\tilde{\nu}_{\text{calc}} = f_1 \tilde{\nu}_1 + f_2 \tilde{\nu}_2 \tag{4}$$

where, f_1 and f_2 are the volume fraction of solvent 1 and solvent 2; $\tilde{\nu}_1$ and $\tilde{\nu}_2$ represent the emission energy of investigated sample in pure solvent 1 and solvent 2.

Usually, the preferential solvation process of a solute are investigated by different solvation parameters, such as the local mole fractions, X_1^L and X_2^L , (Eqs. (5) and (6)), index of preferential solvation, δ_{S2} , (Eq. (7)) and preferential

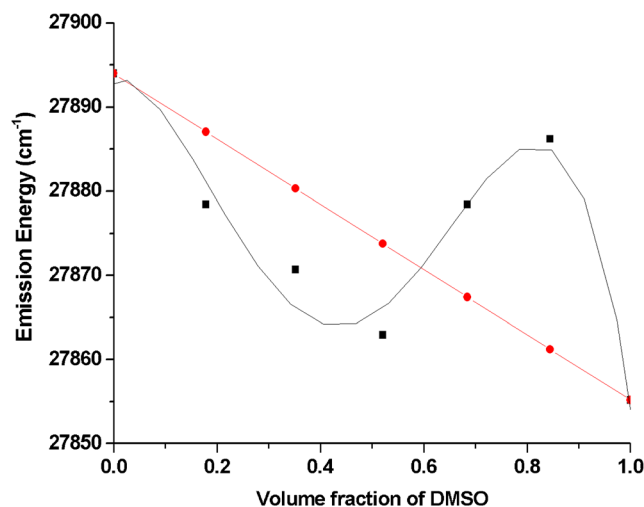


Fig. 9 Plots of emission energy (cm^{-1}) of 9F-Ox as a function of volume fraction of DMF in chloroform-N,N-dimethylformamide (DMF) mixture (---●--- calculated emission energy (ideal solvation) and -■- observed (experimental values) emission energy)

Table 1 The collisional quenching constants and R²coefficient of determination for investigated polymer solutions by metal oxide NPs

Samples	K _{SV}	R ²	% quenching (at 1550 μL NPs)	X = [C _D]/[C _A]
BisF-Ox/SnO ₂	1.07 × 10 ⁸	0.983	66.89	8.20
BisF-Ox/NiO	1.79 × 10 ⁹	0.992	36.71	3.96
BisF-Ox/SnO ₂ / NiO	1.57 × 10 ⁸	0.966	35.41	3.64
6F-Ox/SnO ₂	1.88 × 10 ⁸	0.993	36.29	4.85
6F-Ox/NiO	18.1 × 10 ⁸	0.996	35.25	5.20
6F-Ox/SnO ₂ / NiO	1.85 × 10 ⁸	0.989	39.63	4.13
Co6F/SnO ₂	1.82 × 10 ⁸	0.995	36.16	–
Co6F/NiO	20.07 × 10 ⁸	0.989	35.80	–
Co6F/SnO ₂ / NiO	2.05 × 10 ⁸	0.988	38.45	–

solvation constant, K₁₂ (Eq. (8)). These parameters are defined by follow equations [26]:

$$X_2^L = \frac{\tilde{\nu}_{12} - \tilde{\nu}_1}{\tilde{\nu}_2 - \tilde{\nu}_1} \quad (5)$$

$$X_1^L + X_2^L = 1 \quad (6)$$

$$\delta_{s2} = X_2^L - X_2 \quad (7)$$

$$K_{12} = \frac{X_1^L/X_2^L}{X_1/X_2} \quad (8)$$

A positive value of δ_{s2} indicates a preference of the investigate solute for solvent 2 over solvent 1, while a negative value of δ_{s2} signifies the opposite [26]. But for values of $K_{12} < 1$ the solute exhibit a preference for solvent 1 over solvent 2 and $K_{12} > 1$ denotes the opposite trend [27].

The analysis of preferential solvation process was performed for excited state of investigated compound because here this compound is more sensitive to solvent environment. The variation of emission maxima as a function of mole fraction of DMSO in DMF-DMSO mixture of sample 9F-Ox was exhibited in Fig. 9 and was found that these values deviate from the ideal behavior. This is due to the environment that surrounding the solute molecules is different from the bulk solution. Addition of small amount of DMSO in system induces a deviation from the calculated ideal binary mixture curve (ideal solvation behavior). In the first region of the preferential solvation curves (Fig. 9, until $X_2 = 0.65$) the bulk and local mole fraction composition are approximately equal.

The plot from Fig. 9, suggests as the DMSO content increased upon $X_2 = 0.65$ the solute are preferentially solvated by solvent 2 (DMSO), (see Table 2). These positive and negative deviation from ideal solvation (dual behavior) were attributed to the specific solute-solvent and solvent-solvent interactions (e.g. hydrogen bonding). Also, the positive values of the excess function (δ_{s2}) for $X_2 < 0.65$, indicate a preference of solute for solvent 2 (DMSO) over solvent 1 (DMF) and the values for $K_{12} > 1$ suggest same thing. A similar preferential solvation behavior was observed for compound 9F-Ox in CHCl₃-DMF binary solvent mixtures. For liquid mixtures corresponding to compositions with $X_2 > 0.65$, opposite trend was observed (the solute molecules are preferentially solvated by solvent 1 over solvent 2).

Table 2 Spectral data and the values of the preferential solvation parameters (calculated from fluorescence data) of sample 9F-Ox in CHCl₃-DMF and DMF-DMSO heterogeneous media

Mixed solvents	X ₂	$\tilde{\nu}_{\text{abs}}^{\text{max}}$ (cm ⁻¹)	$\tilde{\nu}_{\text{fl}}^{\text{max}}$ (cm ⁻¹)	SS (cm ⁻¹)	% LMPC	X ₂ ^L	δ _{s2}	K ₁₂
CHCl₃-DMF	0	33,112.58	27,932.96	5179.62	–	–	–	–
	0.172	33,134.52	27,909.57	5224.95	69.57	0.60	0.42	7.22
	0.342	33,167.49	27,901.78	5265.71	42.21	0.80	0.45	7.70
	0.509	33,222.59	27,905.67	5316.91	07.84	0.70	0.19	2.24
	0.675	33,189.51	27,917.36	5272.15	37.89	0.40	- 0.27	0.32
	0.838	33,222.59	27,917.36	5305.23	15.68	0.40	- 0.43	0.12
	1	33,222.59	27,894.00	5328.59	–	–	–	–
DMF-DMSO	0	33,112.58	27,894.00	5218.58	–	–	–	–
	0.178	33,134.52	27,878.45	5256.07	59.29	0.20	0.02	1.15
	0.351	33,167.49	27,870.68	5296.81	37.60	0.40	0.04	1.22
	0.520	33,222.59	27,862.91	5359.67	04.13	0.80	0.27	3.68
	0.684	33,189.51	27,878.45	5311.06	30.01	0.60	- 0.08	0.69
	0.844	33,222.59	27,886.22	5336.37	16.54	0.40	- 0.44	0.12
	1	33,222.59	27,855.15	5367.44	–	–	–	–

Information on the repartitioning of the polar solvent in the vicinity of the solute (fluorophore) has a prominent role in future properties of the investigated system. Thus, quantitatively the polar component from a binary solvent mixtures which surrounding the solute (%LMPC) compared to the bulk composition of the system can be evaluated taking into account to the values of the Stokes shifts, (SS , cm^{-1}) in homogeneous (pure polar and nonpolar solvents) and heterogeneous media (solvent mixtures) and Eq. (9), [28]:

$$\%LMPC = \frac{(SS_{\text{polar}} - SS_{\text{mixture}})}{(SS_{\text{polar}} - SS_{\text{mixture}}) + (SS_{\text{mixture}} - SS_{\text{nonpolar}})} \quad (9)$$

where, the subscripts “nonpolar”, “polar” and “mixture” denote the Stokes shift (in cm^{-1}) in the pure nonpolar, polar and binary solvent mixtures, respectively.

The values of Stokes shifts are easily affected by increased the system polarity (increases amount of the polar solvent from system, Table 2). While, the values obtained of %LMPC for sample 9F-Ox in CHCl_3 -DMF and DMF-DMSO heterogeneous media (Table 2) decreases when as the ratio of DMF or DMSO were increased, excepting at CHCl_3 -DMF ratios of 3–3 (the equilibrium composition) when %LMPC has low value (7.84 and 4.13 %) for both solvent mixtures.

Conclusions

In this paper we investigated the effects of the metal oxide (SnO_2 , NiO and SnO_2/NiO) nanoparticles on the optical properties of some fluorinated poly(1,3,4-oxadiazole-ether)s. UV absorption spectra of these polymers in presence of metal oxide nanoparticles shows enhancement in the absorbance signal. Instead, the emission signals The weak interactions between investigated fluorinated poly(1,3,4-oxadiazole-ether)s and metal oxide nanoparticles was confirmed by non-linear plot of Benesi–Hildebrand equation. The photophysical behavior in heterogeneous media CHCl_3 -DMF and DMF-DMSO has been investigated for excited state of sample 9F-Ox. The optical properties was sensitive to compositions of the investigated heterogeneous environments.

References

- Tao Y, Wang Q, Shang Y, Yang C, Ao L, Qin J, Ma D, Shua Z (2009) Multifunctional bipolar triphenylamine/oxadiazole derivatives: highly efficient blue fluorescence, red phosphorescence host and two-color based white OLEDs. *Chem Commun* 1:77–79. doi:10.1039/b816264f
- Hamciuc C, Hamciuc E, Ipate A, Cristea M, Okrasa L (2009) Thermal and electrical properties of copoly(1,3,4-oxadiazole-ethers) containing fluorene groups. *J Appl Polym Sci* 113:383–391. doi:10.1002/app.30007
- Dhara MG, Banerjee S (2010) Fluorinated high-performance polymers: poly (arylene ether) s and aromatic polyimides containing trifluoromethyl groups. *Prog Polym Sci* 35:1022–1077. doi:10.1016/j.progpolymsci.2010.04.003
- Sun YM (2001) Synthesis and optical properties of novel blue light-emitting polymers with electron affinitive oxadiazole. *Polymer* 42:9495–9504. doi:10.1016/S0032-3861(01)00495-5
- Kwak JK, Park KH, Yun DY, Lee DU, Kim TW (2010) Microstructural and optical properties of SnO_2 nanoparticles formed by using a solvothermal synthesis method. *J Korean Phys Soc* 57(6):1803. doi:10.3938/jkps.57.1803
- Kamaraj P, Vennila R, Arthanareeswari M, Devikala S (2014) Biological activities of tin oxide nanoparticles synthesized using plant extract. *World J Pharm Pharm Sci* 3(9):382–388
- Ayeshamariam A, Meera T, Jayachandran B, Kumar P, Bououdina M (2013) Green synthesis of nanostructured materials for antibacterial and antifungal activities. *Int J Bioassays* 02(01):304–311
- Erkan A, Bakir U, Karakas G (2006) Photocatalytic microbial inactivation over Pd doped SnO_2 and TiO_2 thin films. *J Photochem Photobiol A* 184(3):313–321. doi:10.1016/j.jphotochem.2006.05.001
- Idota Y, Kubota T, Matsufuji A, Maekawa Y, Miyasaka T (1997) Tin-based amorphous oxide: a high-capacity lithium-ion-storage material. *Science* 276(5317):1395–1397. doi:10.1126/science.276.5317.1395
- Dulkeith E, Morteaux AC, Niedereichholz T, Klar TA, Feldmann J, Levi SA, van Veggel FC, Reinhoudt DN, Möller M, Gittins DI (2002) Fluorescence quenching of dye molecules near gold nanoparticles: radiative and nonradiative effects. *Phys Rev Lett* 89:203002. doi:10.1103/PhysRevLett.89.203002
- Kitson SC, Barnes WL, Sambles JR (1995) Surface-plasmon energy gaps and photoluminescence. *Phys Rev B Condens Matter* 52:1441. doi:10.1103/PhysRevB.52.1441
- Szmackinski H, Lakowicz JR, Johnson ML (1994) Fluorescence lifetime imaging microscopy: homodyne technique using high-speed gated image intensifier. *Methods Enzymol* 240:723–748
- Pompa PP, Martiradonna L, Torre AD, Sala FD, Manna L, Vittorio MD, Calabi F, Cingolani R, Rinaldi R (2006) Metal-enhanced fluorescence of colloidal nanocrystals with nanoscale control. *Nat Nanotechnol* 1(2):126–130. doi:10.1038/nnano.2006.93
- Ipate AM, Homocianu M, Hamciuc C, Airinei A, Bruma M (2014) Photophysical behavior of some aromatic poly(1,3,4-oxadiazole-ethers) derivatives. *Spectrochim Acta A Mol Biomol Spectrosc* 123:167–175. doi:10.1016/j.saa.2013.12.057
- Homocianu M, Ipate AM, Hamciuc C, Airinei A (2015) Environment effects on the optical properties of some fluorinated poly(oxadiazole ether)s in binary solvent mixtures. *J Lumin* 157:315–320. doi:10.1016/j.jlumin.2014.09.009
- Pascariu Dorneanu P, Airinei A, Olaru N, Homocianu M, Nica V, Doroftei F (2014) Preparation and characterization of NiO, ZnO and NiO–ZnO composite nanofibers by electrospinning method. *Mat Chem Phys* 148:1029–1035. doi:10.1016/j.matchemphys.2014.09.014
- Tazikeh S, Akbari A, Talebi A, Talebi E (2014) Synthesis and characterization of tin oxide nanoparticles via the Co-precipitation method. *Mat Sci-Poland* 32(1):98–101. doi:10.2478/s13536-013-0164-y
- Kottmann JP, Martin OJF, Smith DR, Schultz S (2001) Dramatic localized electromagnetic enhancement in Plasmon resonant nanowires. *Chem Phys Lett* 341:1–6. doi:10.1016/S0009-2614(01)00171-3
- Gu F, Wang SF, Lu MK, Zhou GJ, Xu D, Yuan DR (2004) Photoluminescence properties of SnO_2 nanoparticles synthesized by sol-gel method. *J Phys Chem B* 108:8119–8123

20. Kavitha SR, Umadevi M, Vanelle P, Terme T, Khoumeri O (2014) Spectral investigations on the influence of silver nanoparticles on the fluorescence quenching of 1,4-dimethoxy-2,3-dibromomethylanthracene-9,10-dione. *Eur Phys J D* 68:308. doi: [10.1140/epjd/e2014-50257-5](https://doi.org/10.1140/epjd/e2014-50257-5)
21. Lakowicz JR (2006) Principles of fluorescence spectroscopy, third edn. Springer, New York, USA
22. Suvetha Rani J, Sasirekha V, Ramakrishnan V (2013) Study of interaction between tin dioxide nanoparticle and 1,4-dihydroxy 2, 3-dimethyl 9,10-anthraquinone sensitizer. *J Lumin* 144:74–78. doi: [10.1016/j.jlumin.2013.06.026](https://doi.org/10.1016/j.jlumin.2013.06.026)
23. Haldar KK, Patra A (2008) Efficient resonance energy transfer from dye to Au@SnO₂ core-shell nanoparticles. *Chem Phys Lett* 462: 88–91. doi: [10.1016/j.cplett.2008.07.068](https://doi.org/10.1016/j.cplett.2008.07.068)
24. Wargnier R, Baranov AW, Maslow VG, Stsipura V, Artemyev M, Pluot M, Sukhanova A, Nabiev I (2004) Energy transfer in aqueous solutions of oppositely charged CdSe/ZnS core/shell quantum dots and in quantum dot – nanogold assemblies. *Nano Lett* 4:451–457. doi: [10.1021/nl0350938](https://doi.org/10.1021/nl0350938)
25. Ipate AM, Hamciuc C, Homocianu M, Musteata VE, Nicolescu A, Bruma M, Belomoina N (2015) Highly fluorinated poly(1,3,4-oxadiazole-ether)s structural, optical and dielectric characteristics. *J Polym Res* 22(95):1. doi: [10.1007/s10965-015-0687-5](https://doi.org/10.1007/s10965-015-0687-5)
26. Umadevi M, Kumari MV, Bharathi MS, Vanelle P, Terme T (2011) Investigations of preferential solvation on 1,4-dimethoxy-3-methyl anthracene-9,10-dione. *Spectrochim Acta A Mol Biomol Spectrosc* 78:122–127. doi: [10.1016/j.saa.2010.09.008](https://doi.org/10.1016/j.saa.2010.09.008)
27. Frankel LS, Langford CH, Stengle TR (1970) Nuclear magnetic resonance techniques for the study of preferential solvation and the thermodynamics of preferential solvation. *J Phys Chem* 74: 1376–1381. doi: [10.1021/j100701a039](https://doi.org/10.1021/j100701a039)
28. Page PM, McCarty TA, Munson CA, Bright FV (2008) The local microenvironment surrounding dansyl molecules attached to controlled pore glass in pure and alcohol-modified supercritical carbon dioxide. *Langmuir* 24:6616–6623. doi: [10.1021/la8005184](https://doi.org/10.1021/la8005184)